

Photoelectrochemical activity of macroporous silicon formed in molten calcium chloride

Eimutis Juzeliūnas^{1,2,3*},

Paul R. Coxon¹,

Derek J. Fray¹,

Putinas Kalinauskas²,

Ignas Valsiūnas²,

Povilas Miečinskas²

¹Department of Materials Science and Metallurgy,
University of Cambridge,
27 Charles Babbage Road,
CB3 0FS Cambridge, United Kingdom

²Institute of Chemistry,
Centre for Physical Sciences and Technology,
A. Goštauto St. 9, Vilnius, Lithuania

³Klaipėda University,
Herkaus Manto St. 84, Klaipėda, Lithuania

A method of macro-porous silicon formation is proposed, which is based on silicon cathodic polarization in molten calcium chloride. It is assumed that the porosity formation is due to interaction of electrochemically reduced calcium metal with the silicon substrate. Surface architectures were composed of the pores up to 10 micrometers in thickness. High photoactivity of the samples was determined by photoelectrochemical measurements using white light and ethyl viologen as an electroactive agent. The proposed method offers new opportunities for silicon surface technologies, for instance, preparation of efficient electrodes for batteries and photoelectrochemical hydrogen generation as well as the platforms for sensors and antireflection coatings for photodevices.

Keywords: porous silicon, molten salts, calcium, etching

INTRODUCTION

Porous silicon due to high surface-to-volume ratio is of interest in various technological fields: optoelectronics, photovoltaics, chemical and biological sensors, biomedical applications and batteries. Nano-porosity improves the light emitting efficiency of silicon due to the quantum confinement effect [1, 2]. Micro-scale texturing of the silicon surface improves the efficiency of photodevices due to light trapping by internal reflection [3, 4]. Porous silicon films are attractive platforms in chemical and biological sensing [3, 5–9]. The platforms make it possible to monitor the refractive index and the photoluminescence effects. Another advantage is chemical functionalization of the surface, which enables recognition of an electroactive substance. Porous silicon sensors were developed for sensing humidity, organic vapour and various gases [9].

Macro-porous silicon has a potential in application for lithium batteries [10–12]. Every silicon atom can accommodate four lithium atoms, which results in a specific insertion capacity of 4200 mA h g⁻¹, which is the highest one among

the lithium alloys. To increase the active area of a silicon anode, several methods were proposed: chemical etching and mechanical grinding [13], formation of a pillar structure by a reactive ion and chemical etching [14–18]. The cost effective methods of silicon of superior capacity, which could replace graphite, are still in great demand.

Silicon electrochemistry in molten salts attracted considerable attention in attempts to extract high-purity silicon from silica [19–27]. The electrochemical deoxidation provides a green alternative to the carbothermic silicon production – a process, which is highly energy inefficient and harmful to the environment. Studies were performed using large-scale precursors such as quartz plates, silica pellets or powders in a container [19–27]. Thin silica layer precursors were studied to obtain surfaces with a specifically high surface area [28]. Of particular interest is the formation of the so-called black silicon – a material with a nano-micro-structured surface, which effectively absorbs visible light [29]. Electrodeposition of a thin silicon layer from a suspension, prepared from silica nanoparticles in molten calcium chloride, has recently also been reported [30].

Silicon surfaces are textured by physical or chemical techniques such as reactive ion etching, laser scribing,

* Corresponding author. E-mail: ejuzel@gmail.com

photolithography and chemical etching. Most of these techniques, however, are costly and include hazardous reactants, such as hydrofluoric acid. Here we show a method of silicon surface structuring in molten calcium chloride at the potentials where calcium metal reduction is possible. The approach is relatively simple, not costly and friendly to the environment.

Photoactivity of silicon is the main characteristic for its use as a solar material. Photoelectrochemical measurements with a liquid junction provide an opportunity to characterize photoactivity of the semiconductor material. It has been shown that photoelectrochemistry provides information, which correlates well with that obtained by the solid-state cells [31]. Thus, there is no need to design a solar cell with a p–n junction to characterize solar energy harvesting. In this paper we studied the photoelectrochemical activity of macroporous silicon using white light illumination and ethyl viologen as the redox agent. The reduction potential of this agent is within the band gap of silicon [30].

EXPERIMENTAL

The molten salt electrolyte was prepared using analytical grade anhydrous CaCl_2 . The salt was kept in an evacuated oven at elevated temperatures to remove residual water and $\text{Ca}(\text{OH})_2$. The residual pressure was 10 ± 5 mBar. The heating pattern involved 3 hours at 80°C and the same duration at 120°C , and finally 18 hours at 180°C .

For voltammetric studies, p-type $\langle 100 \rangle$ single-crystal silicon wafers were used, which diameter was 5 cm, geometric area 22.8 cm^2 , thickness 275 ± 25 micron and resistivity 1 to 30 ohm cm^{-1} . The samples were thermally coated by a silica layer of 10 nm thickness (from Si-Mat GmbH, Germany). One side of the specimens was polished. Rectangular specimens $3 \times 1\text{ cm}$ were cut from the wafers using a diamond knife. The upper part of the specimen was attached to a molybdenum wire (0.5 mm) frame and the sample has been immersed into molten salt so that only silicon contacted the electrolyte. By doing so, we obtained the voltammetric data, which relate solely to silicon electrochemistry with no contribution of the Mo current collector.

Macroporous silicon was formed using the wafers with a 100 nm thermal silica layer as the precursors. The samples were attached to a molybdenum frame as described previously [28, 29] and placed into the crucible.

A cylindrical alumina crucible was used, which was placed inside a stainless steel reactor in a vertical tube furnace (Instron SFL, UK). The melted salt was held at 850°C . The depth of the electrolyte in the crucible was about 5 cm. Argon gas was supplied constantly in the reactor during the melting procedure and subsequent experiments. Graphite cylindrical rods, 10 mm in diameter, served both as pseudo-reference and counter electrodes. All potentials are given throughout the paper with reference to the graphite pseudo-reference electrode. After the sample was cooled down, it has been rinsed in deionised water to dissolve the adherent calcium chloride, which is a well

soluble salt. The sample was kept afterwards in a hydrochloric acid solution (pH 1) to dissolve possible contaminants.

Photoelectrochemical measurements were carried out in a glass cell equipped with a quartz window for sample illumination. A white LED has been used as an illumination source. The electrolyte was 0.1 M KCl containing 0.05 M ethyl viologen diperchlorate (Sigma Aldrich) as the redox agent.

RESULTS AND DISCUSSION

Figure 1 shows the cyclic voltammetry measurement for silicon electrode in molten CaCl_2 at 850°C . A thin native oxide layer is a typical component on silicon, which spontaneously forms in ambient atmosphere and during the surface treatments such as polishing in slurry. Figure 1 relates to a well-defined silicon precursor with a 10 nm thermal SiO_2 layer. Note that the surface oxidation is usually applied to improve electronic properties of silicon – the oxygen reduces the number of dangling bonds on the surface.

Most of silicon electrochemical studies in molten salts were performed using complex electrodes composed of Si, SiO_2 and a metal collector (Mo, Ni, W) [19–28]. The metal (Me) current collector is attached to Si to induce the reduction. It means that four phases are in contact: Me–Si– SiO_2 – CaCl_2 . This makes it difficult to study electrochemical mechanisms because it is difficult to differentiate between the current contributions by individual phases. Figure 1 shows the cyclic voltammogram with no contribution from a foreign current collector due to the applied experimental configuration, as described in the experimental section. Several distinctive features are characteristic of the studied system. The current peak at the initial electrode polarization (A, Fig. 1) could be attributed to: 1) reduction of a silica layer; 2) a background current, which is typical for the molten salt electrolyte due to its electronic conductivity; and 3) reduction of some contaminants. An increase in the cathodic current below -0.5 V indicates the calcium reduction

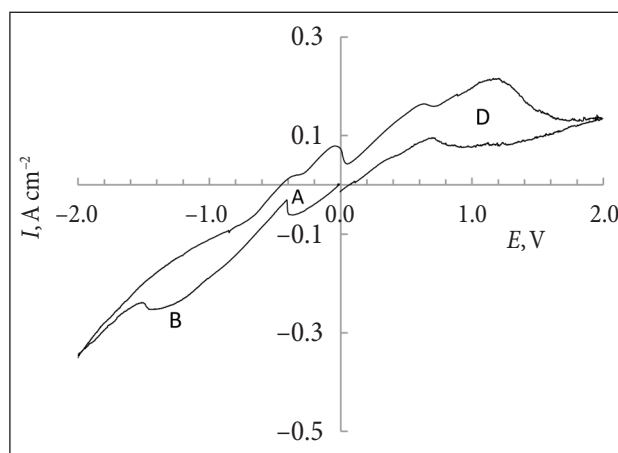


Fig. 1. Cyclic voltammogram recorded for silicon with a 10 nm SiO_2 layer in molten CaCl_2 at 850°C and a potential sweep rate of 100 mV s^{-1} . The curve was started from the zero-current point in the negative direction

$\text{Ca}^{2+} + 2e^- \rightarrow \text{Ca}$. The reduced calcium may interact with silicon producing silicides $n\text{Ca} + m\text{Si} \rightarrow \text{Ca}_n\text{Si}_m$. The silicides, due to less electric conductivity, may cause appearance of the current peak B. Note that a common method of silicide production is the reaction between calcium gas (G) and solid (S) silicon in inert atmosphere at $T = 850^\circ\text{C}$: $2\text{Ca}_g + \text{Si}_s \rightarrow \text{Ca}_2\text{Si}_g$ [32].

The anodic peak C in Fig. 1 is due to calcium oxidation. The wide anodic area with a limiting current (not increasing one) relates to the oxidation of silicon $\text{Si} - 2e^- \rightarrow \text{Si}^{2+}$. Formation of pores and evolution of silicon tetrachloride gas (SiCl_4) inside the pores are the first hypothesis to explain the passive behaviour of the electrode. Electrochemistry of the SiCl_4 -Si process in the molten salt electrolyte was first studied by Matsuda et al. [33]. Also, generation of chlorine gas is possible in the far anodic region.

The melting point of calcium $T_m = 839^\circ\text{C}$ is slightly below the operating temperature of our experiment, which is $T = 850^\circ\text{C}$. Therefore, calcium metal could be reduced in a liquid phase. Six main phases of silicides are known: CaSi_2 , $\text{Ca}_{14}\text{Si}_{19}$, Ca_3Si_4 , CaSi , Ca_2Si_3 and Ca_2Si [32]. The melting points of these compounds are in the range 700 to 935°C . Thus, in our experiments, silicides could form in a liquid phase as well.

Chronoamperograms in Fig. 2 show the current variation when polarizing the electrodes down to the potentials, at which calcium reduction occurs and silicide formation is possible (-0.9 and -1.25 V). A current maximum is typical of the initial stage of polarization (curves 2 and 3). The subsequent limiting current indicates electrode passivation, most probably, due to formation of a less conductive interface $\text{Si}-\text{Ca}_n\text{Si}_m-\text{Ca}$. No such behaviour is observed on the molybdenum electrode (curve 1, Fig. 2). It means that Ca is reduced preferentially on Si when using the Mo-Si system as an electrode. Potentiodynamic measurements showed an onset of Ca reduction current on Mo at $E_{\text{Ca}/\text{Ca}^{2+}} \sim -1.3$ V, which is much less when compared to silicon (Fig. 1).

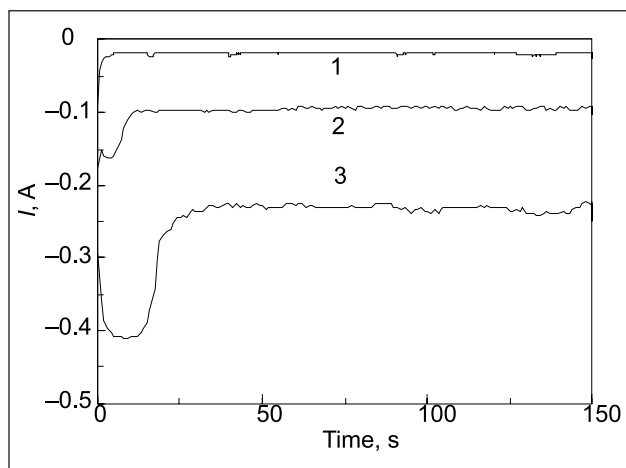


Fig. 2. Chronoamperometric plots: 1 is background current on a Mo wire frame, electrolyte contacting area $S = 2\text{ cm}^2$, $E = -1.25$ V vs graphite; 2 is a rectangular Si sample with a native oxide in the Mo frame, $S = 3\text{ cm}^2$, $E = -0.9$ V; 3 is silicon wafer with native oxide in the Mo frame, $S = 22\text{ cm}^2$, $E = -1.25$ V

A porous structure develops on silicon substrate in the cathodic region of calcium deposition as demonstrated

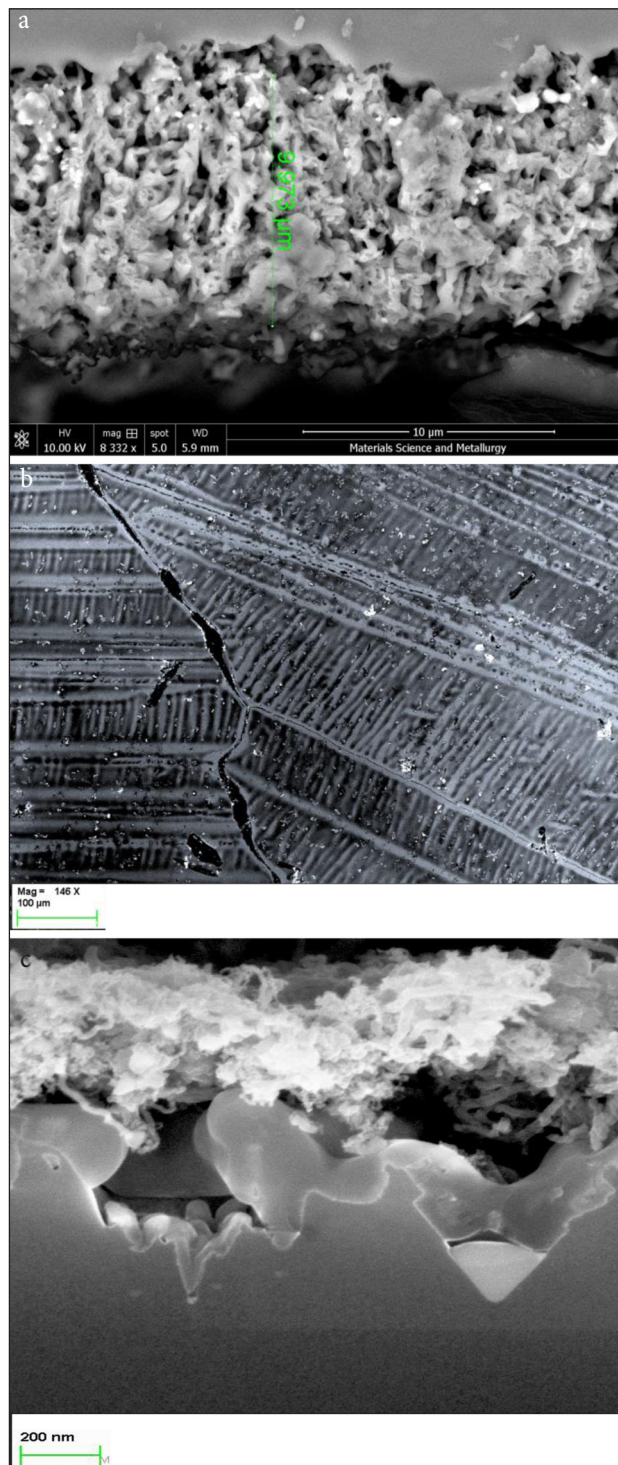


Fig. 3. SEM images: a is a cross-section of the sample formed on silicon substrate (top) by polarization in molten CaCl_2 at $E = -0.9$ V vs graphite for 3 hours. Precursor is silicon wafer with 100 nm thermal oxide; b is a surface view at the initial stage of polarization ($E = -1.0$ V, 1 min) of the precursor with a 2 μm silica layer. A nano-fiber structure on the top covers the pores with frozen liquid inside, which identify an etching process; c is a cross-section of the surface obtained at $E = -1.0$ V, $t = 18$ min using the precursor with a 2 μm silica layer

by the cross-section in Fig. 3a. The sample has been kept at $E = -0.9$ V for 3 hours. The obtained rather thick macro-porous layer (~ 10 μm) indicates silicon dissolution with distinctive localization of the process. The developed layer is much thicker than the silica layer on the precursor (0.1 μm) so it cannot be attributed to silicon reduction from the silica layer. The pore size is of the order of micrometers, thus, they could be ascribed to macropores (according to the IUPAC classification, the micropores are those below 2 nm in diameter, the mesopores in the range 2 to 50 nm and the macropores greater than 50 nm).

When polarizing the Si-SiO₂ precursor with an attached Mo current collector, silica deoxidation starts at the three-phase interface Mo-SiO₂-CaCl₂: $\text{SiO}_2 + 4e^- \rightarrow \text{Si} + 2\text{O}^{2-}$ [19–29]. The reduced silicon forms a new interface Si-SiO₂-CaCl₂, which outspreads over the silica surface due to silica conductivity at a high temperature. Figure 3b maps the reaction pathways during the initial stage of polarization ($t = 1$ min). A network structure is observed, which is actually a system of filament-like microelectrodes. Calcium reduction may occur on such conductive network transforming subsequently to a less conductive silicide network. The latter forms a kind of template, which will be inherited by the Si substrate.

The silicon surface etching is also demonstrated by the cross section in Fig. 3c. The precursor was Si-2 μm SiO₂. Silica is reduced, as discussed above, by forming a fine nanofiber structure on the top of the sample. The dendritic structure is typical of the electrochemical reduction of quartz [19]. Figure 3c identifies development of the pits, whose size is of the order of hundreds of nanometers. Globular formations, which have a shape of a frozen liquid, confine the void spaces and they are also seen on the bottom of the pits identifying an etching process. The XRD study identified Si, CaSi₂ and Ca₂Si on the surface (these data are not given here).

Figure 4 shows the photopotential variation at the open circuit when illumination is switched periodically on and off. The potential increases rapidly when illumination is switched

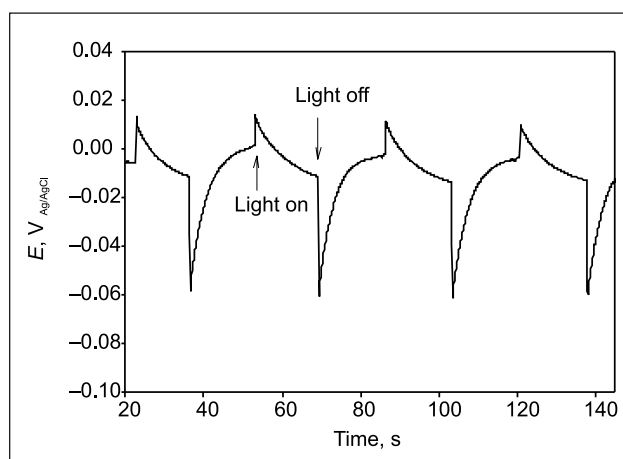


Fig. 4. E_{opp} variation in 0.1 M KCl + 0.05 methyl viologen during white light illumination $N = 70$ mW cm^{-2} and in the darkness for silicon wafer with a native 0.8 nm oxide layer

on and then drops down rather slowly. The initial photo-peak is due to generation of holes in the p-type sample. The subsequent negative shift is caused by a balancing of the surface charge by electrolyte anions. A vice-versa process takes place when illumination is switched off: a rapid negative potential shift due to termination of charge generation and desorption of the anions. A quite different behaviour exhibits the sample treated in molten salt (Fig. 5). The open circuit potential of this electrode is less when compared to that of the untreated sample (Fig. 4). The positive photo-response indicates a p-type semiconducting surface. Much slower induction-relaxation periods are observed and the photo-response is much greater (about 50 mV). Such behaviour implies high photoactivity due to internal light trapping by the porous structure. High photoactivity is also evident from the cathodic currents of viologen reduction (Fig. 6). Very low current is observed for untreated silicon wafer (curve 1). The sample treated in molten salt shows a higher current, which is most probably

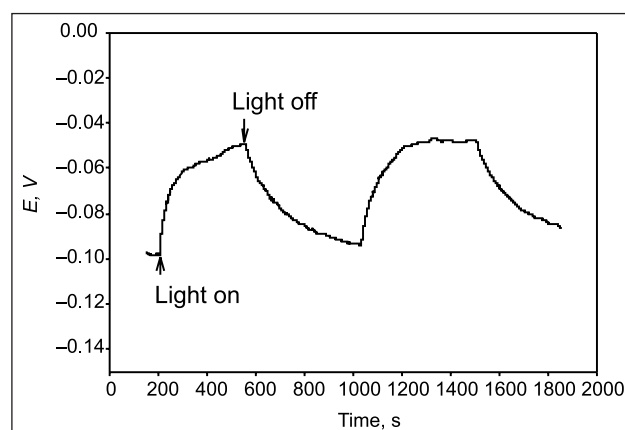


Fig. 5. E_{opp} variation in 0.1 M KCl + 0.05 methyl viologen during white light illumination $N = 70$ mW cm^{-2} and in the darkness for the macro-porous sample formed on silicon by polarization in molten CaCl₂ at $E = -0.9$ V for 3 hours (Fig. 3a)

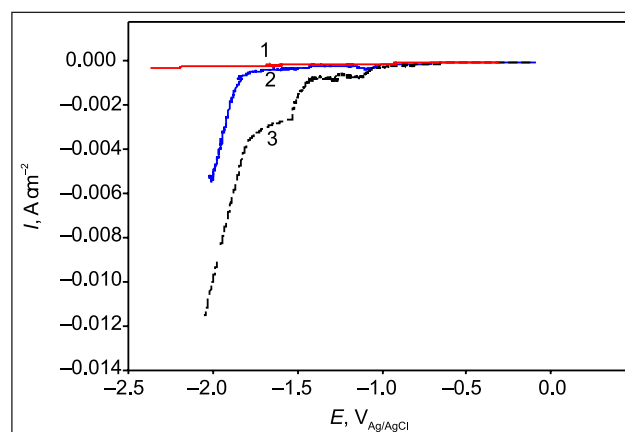


Fig. 6. Cathodic polarization curves obtained in 0.1 M KCl + 0.05 methyl viologen at potential scan rate 10 mV s^{-1} for silicon wafer (1), the sample treated in molten salt as shown in Fig. 3a (2) and an analogous experiment applying white light illumination $N = 70$ mW cm^{-2}

caused by a larger surface area (curve 2). Such current increases by one order of magnitude when illumination is applied (curve 3).

High photo-activity of the obtained silicon structures shows its potential to be applied for effective light harvesting. The structures are promising to be applied as antireflection coatings. The reflectance spectroscopy showed that the samples shown in Fig. 3 absorbed up to 95% of the light in a wide range of wavelength from 450 to 1000 nm. In this respect, it is important to note that silicon nanospheres were shown to be effective light-harvesters improving both quantum and conversion efficiencies [34]. The effect has been explained by a strong forward scattering of the light. Thus, development of new methods of formation of nano-micro-spherical structures on silicon, as this paper demonstrates, is of increasing technological interest.

CONCLUSIONS

Macroporous silicon structures with pore thickness of the order of micrometers were formed on the silicon substrate using silicon-silica precursors and electrochemical polarization in molten CaCl_2 in the potential region where calcium reduction is possible. Photoelectrochemical measurements indicated high photo-activity of the samples. The obtained porous structures are promising in various applications where high surface-to-volume ratio is of importance: antireflection coatings for photovoltaic devices, batteries, or platforms for sensors.

ACKNOWLEDGEMENTS

The research leading to these results has received funding from the European Community's Seventh Framework Programme [FP7/2007-213] under grant agreements No. 235272 and PEOF-GA-2011-300501.

Received 20 October 2015
Accepted 30 November 2015

References

1. R. T. Collins, P. M. Fauchet, M. A. Tischler, *Phys. Today*, **50**(1), 24–31 (1997).
2. L. T. Canham, *Appl. Phys. Lett.*, **57**, 1046 (1990).
3. P. Singh, S. N. Sharma, N. M. Ravindra, *JOM*, **62**, 15–24 (2010).
4. J. Szlufcik, G. Agostinelli, F. Duerinckx, E. Van Kerschaver, G. Beaucarne, in: T. Markvart, L. Castauer (eds.), *Solar Cells: Materials, Manufacture and Operation*, p. 91, Elsevier Ltd. (2005).
5. A. Jane, R. Dronov, A. Hodges, N. H. Voelcker, *Trends Biotechnol.*, **27**, 230 (2009).
6. K. A. Kilian, T. Böcking, J. J. Gooding, *Chem. Commun.*, **6**, 630 (2009).
7. E. J. Anglin, L. Cheng, W. R. Freeman, M. J. Sailor, *Adv. Drug Delivery Rev.*, **60**, 1266 (2008).
8. J. Salonen, A. M. Kaukonen, J. Hirvonen, V. P. Lehto, *J. Pharm. Sci.*, **97**, 632 (2008).
9. S. Ozdemir, J. L. Gole, *Current Opinion in Solid State and Materials Science*, **11**, 92 (2007).
10. Patent WO2010/040985, 2010.
11. U. Kasavajjula, C. Wang, A. J. Appleby, *J. Power Sources*, **163**, 1003 (2007).
12. M. Winter, J. O. Besenhard, M. E. Spahr, P. Novak, *Adv. Mater.*, **10**, 725–763 (1998).
13. T. Takamura, S. Ohara, M. Uehara, J. Suzuki, K. Sekine, *J. Power Sources*, **129**, 96 (2004).
14. Patent GB2395059A.
15. Patent US-7033936.
16. K. Peng, Y. Wu, H. Fang, X. Zhong, Y. Xu, J. Zhu, *Angew. Chem. Int. Ed.*, **44**, 2737 (2005).
17. Patent WO2007/083152.
18. Patent WO2009/010758.
19. T. Nohira, K. Yasuda, Y. Ito, *Nat. Mater.*, **2**, 397 (2003).
20. X. Jin, P. Gao, D. Wang, X. Hu, G. Z. Chen, *Angew. Chem. Int. Ed.*, **43**, 733 (2004).
21. K. Yasuda, T. Nohira, K. Amezawa, Y. H. Ogata, Y. Ito, *J. Electrochem. Soc.*, **152**, D69 (2005).
22. K. Yasuda, T. Nohira, Y. Ito, *J. Phys. Chem. Solids*, **66**, 443 (2005).
23. P. C. Pistorius, D. J. Fray, *J. S. Afr. Inst. Min. Metall.*, **106**, 31 (2006).
24. W. Xiao, X. Jin, Y. Deng, D. Wang, X. Hu, G. Z. Chen, *Chem. Phys. Chem.*, **7**, 1750 (2006).
25. K. Yasuda, T. Nohira, R. Hagiwara, Y. H. Ogata, *Electrochim. Acta*, **53**, 106 (2007).
26. S.-C. Lee, J.-M. Hur, C.-S. Seo, *J. Ind. Eng. Chem.*, **14**, 651 (2008).
27. W. Xiao, X. Jin, Y. Deng, D. Wang, G. Z. Chen, *J. Electroanal. Chem.*, **639**, 130 (2010).
28. E. Juzeliunas, A. Cox, D. J. Fray, *Electrochem. Commun.*, **12**, 1270 (2010).
29. E. Juzeliunas, A. Cox, D. J. Fray, *Electrochim. Acta*, **68**, 123 (2012).
30. S. K. Cho, F.-R. F. Fan, A. J. Bard, *Angew. Chem. Int. Ed.*, **51**, 12740 (2012).
31. H. Ye, H. S. Park, V. Akhavan, et al., *J. Phys. Chem. C*, **115**, 234 (2011).
32. R. Ropp, *Encyclopedia of the Alkaline Earth Compounds*, Elsevier, 375 (2013).
33. T. Matsuda, S. Nakamura, K. Ide, K. Nyudo, S. J. Yae, Y. Nakato, *Chem. Lett.*, **7**, 569 (1996).
34. G.-J. Lina, H.-P. Wanga, D.-H. Liena, et al., *Nano Energy*, **6**, 36 (2014).

Eimutis Juzeliūnas, Paul R. Coxon, Derek J. Fray,
Putinas Kalinauskas, Ignas Valsiūnas, Povilas Miečinskas

**MAKROPORĖTO SILICIO, SUFORMUOTO
IŠLYDYTAME KALCIO CHLORIDE,
FOTOELEKTROCHEMINIS AKTYVUMAS**

S a n t r a u k a

Pasiūlytas makroporėto silicio formavimo metodas, atliekant silicio katodinį poliarizavimą išlydytame kalcio chlorido elektrolite. Manoma, kad paviršiaus porėtumas susidaro dėl elektrochemiškai redukuoto kalcio sąveikos su silicio substratu. Gautos įvairios paviršiaus struktūros, kurias sudaro iki 10 mikrometrų diametro poros. Fotoelektrocheminiais matavimais nustatytas didelis pavyzdžių fotoaktyvumas. Matavimai atlikti chloridiniame elektrolite, panaudojant elektroaktyvų agentą – etilo viologeną. Pasiūlytas metodas atveria naujas silicio paviršiaus technologijų galimybes, pavyzdžiui, efektyvių silicio elektrodų gamybą elektros baterijoms, fotoelektrocheminį vandenilio generavimą, jutiklių platformas ar fotoįrenginių antiatspindžio dangas.